2001

Application of Dynamic System Identification to Timber Beams - part I

S T. Peterson
Washington State University

D I. McLean
Washington State University

M D. Symans
Washington State University

David Pollock
George Fox University, dpollock@georgefox.edu

W F. Cofer
Washington State University

See next page for additional authors

APPLICATION OF DYNAMIC SYSTEM IDENTIFICATION TO TIMBER BEAMS. I

By S. T. Peterson,[1] D. I. McLean,[2] M. D. Symans,[3] D. G. Pollock,[4] W. F. Cofer,[5] R. N. Emerson,[6] and K. J. Fridley[7]

ABSTRACT: In this first part of a two-part paper, development of a method of dynamic system identification for timber beams is presented with an analytical verification of the method using a finite-element model. A method of global nondestructive evaluation for identifying local damage and decay in timber beams is investigated in this paper. Experimental modal analysis is used in conjunction with a previously developed damage localization algorithm. The damage localization algorithm utilizes changes in modal strain energy between the mode shapes of a calibrated model, representing the undamaged state of the beam of interest, and the experimentally obtained mode shapes for a timber beam. Analytical evaluations were performed to demonstrate and verify the use of this method of global nondestructive evaluation for the localization of damage or decay in timber beams. In a companion paper, experimental laboratory tests are presented that verify the use of dynamic system identification to locate damage within timber beams.

INTRODUCTION

Nondestructive evaluation (NDE) of wood is the science and art of determining the material properties and/or structural capacity of individual members or for an entire timber structure without impairing the member or structure in its usefulness for its intended purpose. A number of methods have been developed and implemented in the field of nondestructive evaluation for wood. These methods include visual inspection, stress wave, drill resistance, radiography, ultrasonics, and deflection/vibration analysis (Emerson et al. 1998).

Many of the methods already developed for the nondestructive evaluation of wood are performed on a very localized scale. Conducting an evaluation of an entire structure using these methods can be very time-consuming and inefficient. It is therefore desirable to develop a method of nondestructive testing for timber structures that can identify damage or decay from a global perspective. The method selected in this study for global evaluation was deflection/vibration analysis, specifically, experimental modal analysis.

Experimental modal analysis is typically defined as the determination of natural frequencies of vibration, mode shapes, and damping ratios from experimental vibration measurements. This method of analysis was selected primarily because of the global nature of the form of evaluation. The effectiveness of experimental modal analysis has been demonstrated in terms of its capability to identify and/or locate damage in steel bridges (Mazurek and DeWolf 1990; Stubbs and Kim 1996a). To perform experimental modal testing, the structure is excited in its modes of vibration and the response is measured at several points within the structure. Impulse excitation was selected over ambient traffic and mass-shaker excitation as the method used to excite the structure since many timber structures are located in remote areas, and this allows the testing equipment to be as simple as possible.

Once the vibration measurements have been made for the structure of interest, the modal parameters must be determined and analyzed to identify possible locations of damage within the structure. There have been a number of methods developed to analyze the modal parameters of a structure to identify and/or locate possible areas of damage (Aktan et al. 1992; Raghavendrachar and Aktan 1992; Stubbs and Kim 1996a). Although changes in the natural frequencies of vibration may determine whether a structure has been damaged, the damage cannot be located within the structure using changes in natural frequencies alone (Alampalli et al. 1992). In this study, mode shapes were the primary modal parameter selected to indicate whether the structure may have been damaged since changes in the mode shapes also have the potential to identify the location of damage within the structure. The method of damage localization used in this study was largely based on methods developed previously for steel plate girders and highway bridges to localize and estimate the severity of damage within the structure (Bolton et al. 1998; Stubbs et al. 1998). Several analytical studies have been published that verify the performance of the damage localization and severity estimation algorithm (Stubbs and Garcia 1996b; Stubbs et al. 1997).

The method outlined above has not been used previously to locate damage or decay within timber structures. To begin the application of experimental modal analysis and the damage localization method to timber structures, analytical studies and laboratory tests are performed on simply supported timber beams. These verification studies are performed to confirm the applicability of the method where natural variability in material properties exists within a timber beam as well as simulated damage. The method will be extended to more complex timber structures in the future.

This paper presents discussion on experimental modal analysis and associated signal processing, background information on the damage localization algorithm, and results from an analytical verification of the approach. A companion paper (Peterson et al. 2001) presents results from laboratory tests using the damage localization algorithm to locate simulated damage in timber beams, and the experimental results are compared with the results from the analytical investigation. Based on the results of the two papers, the effectiveness of using a global nondestructive evaluation method for identifying damage in timber beams will be demonstrated.

[1]Grad. Student, Dept. of Civ. and Envir. Engrg., Washington State Univ., Pullman, WA 99164-2910.
[2]Prof., Dept. of Civ. and Envir. Engrg., Washington State Univ., Pullman, WA 99164-2910.
[3]Asst. Prof., Dept. of Civ. and Envir. Engrg., Washington State Univ., Pullman, WA 99164-2910.
[4]Asst. Prof., Dept. of Civ. and Envir. Engrg., Washington State Univ., Pullman, WA 99164-2910.
[5]Assoc. Prof., Dept. of Civ. and Envir. Engrg., Washington State Univ., Pullman, WA 99164-2910.
[6]Asst. Prof., School of Civ. and Envir. Engrg., Oklahoma State Univ., Stillwater, OK 74078-5033.
[7]Prof., Dept. of Civ. and Envir. Engrg., Washington State Univ., Pullman, WA 99164-2910.

SIGNAL PROCESSING AND DETERMINATION OF MODAL PARAMETERS

Impact vibration tests are performed by impacting a structure with an instrumented impact hammer and measuring the acceleration response at several points within the structure. The acceleration response is measured at a sufficient number of points along the span so that the mode shapes can be accurately reconstructed through interpolation (Stubbs and Park 1996c).

The maximum frequency sufficiently excited in the structure by the impulse excitation is referred to as the cutoff frequency. The cutoff frequency ω_c approximately corresponds to the point at which the magnitude of the frequency spectrum of the impulse signal drops 10 or 20 dB below its maximum value (Inman 1996). At frequencies higher than ω_c, the test structure does not receive enough energy to sufficiently excite the associated natural modes of vibration. Thus, the cutoff frequency is used to determine the useful range of modal frequencies excited in the beam.

Impact force and acceleration response should be recorded at a sampling frequency F_s twice that of either the highest natural frequency of vibration of interest or the highest frequency sufficiently excited by the impulse excitation, i.e., the cutoff frequency. The sampling frequency requirement is based on two effects of signal processing. First, in performing a Fourier transform to examine the recorded data in the frequency domain, the useful range of frequency domain data will range from zero to the Nyquist frequency ($F_s/2$). Secondly, aliasing problems in the measured response can be avoided if the sampling frequency is at least equal to twice the highest frequency sufficiently excited, since the aliased data will then fall in a range above the useful range of the input excitation.

The natural frequencies and mode shapes are obtained from the recorded time domain data by evaluating the frequency response function (FRF) for each measurement point. The FRF is defined as the ratio of the Fourier transforms of the output and input signals. However, better results are obtained in practice by evaluating the FRF as the ratio of the cross-spectrum between the input and output to the power spectrum of the input signal (Halvorsen and Brown 1977). Specifically, this method minimizes the effects of noise associated with the output. The FRF $H(\omega)$ was calculated as follows:

$$H(\omega) = \frac{G_{uv}(\omega)}{G_u(\omega)} \tag{1}$$

where $G_{uv}(\omega) = U^*(\omega)V(\omega)$, cross-spectrum between $u(t)$ and $v(t)$; $G_u(\omega) = U^*(\omega)U(\omega)$, power spectrum of $u(t)$; $V(\omega)$ = Fourier transform of $v(t)$; $U(\omega)$ = Fourier transform of $u(t)$; $U^*(\omega)$ = complex conjugate of $U(\omega)$; $u(t)$ = input or excitation signal; and $v(t)$ = output or response signal.

Data windowing is commonly used in signal processing to reduce noise in the recorded time domain data or to allow the time domain signal to be more accurately converted into the frequency domain via the Fourier transform. An exponential window is applied to the acceleration data, i.e., the output $v(t)$, to make the signal appear more periodic, thus improving the results of the Fourier transformation $v(\omega)$. A rectangular window is applied to the impact force data to remove the noise recorded when the impact hammer is not in contact with the beam, thus improving the results of the Fourier transformation of the input signal $u(\omega)$. The window functions are applied to the time domain signals prior to calculating the FRF. The natural frequencies of vibration of the beam are identified as spikes in the plot of the amplitude of the FRF. These spikes in the amplitude of the FRF indicate resonance in the beam response.

The amplitude of the spike in the FRF at frequency ω_i for measurement location j is proportional to the modal coordinate ϕ_{ij} for location j in mode shape i. The mode shape coordinates ϕ_{ij} along the span of the beam (i.e., for all j) for mode i are entered into a column vector. This vector then defines the mode shape of the beam for mode i corresponding to the natural frequency of vibration ω_i.

For a given sampling location, the amplitudes of the mode shape coordinates will vary from one test to the next due to the variation in applied impulse force. The mode shape coordinates are normalized by dividing the mode shape coordinates by the euclidean norm of the respective mode shape vector. This is done to minimize the variation in amplitude so that more consistent mode shapes can be obtained. To reduce the effect of errors in measuring the experimental mode shapes, the normalized mode shape vectors from several tests are averaged.

The FRF $H(\omega)$ will likely indicate that there are several frequencies adjacent to the dominant natural frequencies of vibration that may appear to correspond to the mode shape of interest. Modal assurance criteria (MAC) values are used to determine which of the possible experimental modes best correlates with the corresponding theoretical mode shape. The theoretical mode shapes can be obtained from a finite-element model that describes the dynamic response of the beam. The MAC values are calculated for each of the possible experimental mode shapes using the following expression:

$$\text{MAC} = \frac{\left(\sum_{j=1}^{n} \phi_{Tj}\phi_{Ej}\right)^2}{\sum_{j=1}^{n} \phi_{Tj}^2 \sum_{j=1}^{n} \phi_{Ej}^2} \tag{2}$$

where ϕ_{Tj} = jth coordinate of the theoretical mode shape; ϕ_{Ej} = jth coordinate of the experimentally obtained mode shape; and n = number of coordinates in the mode shape vectors. The MAC values will range from 0 to 1.0 (0 indicating no correlation with the theoretical mode shape, and 1.0 indicating perfect correlation with the theoretical mode shape).

Experimentally obtained mode shape vectors will have as many coordinates as locations at which the acceleration was measured along the span of the beam. Values between the experimentally measured mode shape coordinates can be interpolated using Shannon's sampling theory to generate mode shape vectors of greater length. The reconstructed mode shape vector is given by the following expression:

$$S(x) = \sum_{n=-\infty}^{\infty} S(nT) \frac{\sin\left\{\pi\left(\frac{x}{T} - n\right)\right\}}{\pi\left(\frac{x}{T} - n\right)} \tag{3}$$

where $S(x)$ = interpolated mode shape coordinate at position x; $S(nT)$ = experimental mode shape coordinates at position nT; T = spacing of the experimental mode shape coordinates; and n = number of coordinates in experimental mode shape vectors.

To avoid truncation errors in reconstructing the mode shapes in the spatial domain, the experimental mode shape vectors should be spatially repeated to obtain better results using Shannon's theory. The interpolated mode shape given by (3) represents the exact reconstruction of the mode shape of interest since the summation is for all n between negative and positive infinity, i.e., for an infinite number of spatially repeated experimental mode shape vectors. Acceptable results can be obtained using several repeats of the experimental mode shape coordinates, i.e., for a finite range of values for n. A more detailed explanation of applying Shannon's sampling theory to reconstruct mode shapes can be found in Park and Stubbs (1995) and in Stubbs and Park (1996c).

DAMAGE LOCALIZATION

To localize the inflicted damage present in the beam of interest in this investigation, a method of damage localization developed previously (Stubbs et al. 1995) was used. The localization method is based on the differences in modal strain energy between an undamaged or pristine structure and that of the damaged structure.

An expression for the modal strain energy stored in the beam for the ith mode of vibration U_i is given below

$$U_i = \frac{1}{2}\int_0^L E(x)I\{\phi_i''(x)\}^2\,dx \tag{4}$$

In this expression, $E(x)$ = modulus of elasticity of the beam that varies along the length for a timber beam; I = second moment of area of the cross section of the beam; and $\phi_i''(x)$ = second derivative of the ith mode shape with respect to the position along the beam (obtained numerically). If the beam is divided into j elements, the modal stain energy concentrated in the jth element for the ith mode is given by

$$U_{ij} = \frac{(EI)_j}{2}\int_j \{\phi_i''(x)\}^2\,dx \tag{5}$$

where the integral is applied over the limits of the jth element only and it is assumed that $E(x)$ is constant over the length of element j. The fraction of modal strain energy for the ith mode, concentrated in the jth element, can be expressed as

$$F_{ij} = \frac{U_{ij}}{U_i} \tag{6}$$

where $0 < F_{ij} < 1.0$. Expressions similar to those given in (4)–(6) can be written for the damaged beam. The damaged state of the beam will be denoted with a superscript asterisk.

To develop an indicator of damage localization, the following approximate expression that relates the behavior of the undamaged structure to that of the damaged structure is used:

$$1 + F_{ij} \cong 1 + F_{ij}^* \tag{7}$$

The fundamental indicator of damage used in the derivation of the damage localization algorithm is the quotient F_{ij}^*/F_{ij} (Stubbs and Garcia 1996b). During the derivation of the algorithm, the axes defining the F_{ij} and F_{ij}^* values are shifted from 0 to -1 to prevent the quotient (F_{ij}^*/F_{ij}) from becoming undefined as F_{ij} approaches 0. This is reflected in the addition of unity to both sides of (7). The condition of F_{ij} approaching 0 will occur if the element is located at the node point of a mode, and simultaneously, as the element size approaches zero (Stubbs and Garcia 1996b). Although the algorithm has been adjusted so that the damage indicator values will no longer become undefined, the algorithm may still be prone to false-positive locations of damage (indicating damage where there is no actual damage in the beam).

The damage indicator for the jth element and the ith mode β_{ij} may then be defined as

$$\beta_{ij} = \frac{1 + F_{ij}^*}{1 + F_{ij}} = \frac{\left[\int_j \{\phi_i''^*(x)\}^2\,dx + \int_0^L \{\phi_i''^*(x)\}^2\,dx\right]\int_0^L \{\phi_i''(x)\}^2\,dx}{\left[\int_j \{\phi_i''(x)\}^2\,dx + \int_0^L \{\phi_i''(x)\}^2\,dx\right]\int_0^L \{\phi_i''^*(x)\}^2\,dx} \tag{8}$$

For brevity here, see Stubbs et al. (1995) for a more thorough derivation of (8). The above expression attempts to quantify changes in stiffness at a given location j by using pre- and postdamage mode shapes. Each of the terms that appear on the right side of the above equation can be measured. Also, each of the mode shape coordinates represents a location along the span of the beam that could possibly be damaged. For this reason, the mode shape vectors are interpolated using Shannon's theory to increase the number of possible damage locations that can be identified.

To account for all available modes NM the damage indicator for a single element j is given as

$$\beta_j = \frac{\sum_{i=1}^{NM} \text{Num}_{ij}}{\sum_{i=1}^{NM} \text{Denom}_{ij}} \tag{9}$$

where Num_{ij} = numerator of β_{ij} in (8); and Denom_{ij} = denominator of β_{ij} in (8).

Based on the approximations and assumptions made in the derivation of the damage localization algorithm, the value of β_j for all j elements is very nearly equal to 1.0. In comparing the damage indicator value for one element with another it is difficult to discern if the β_j values indicate damage at the jth element. Thus, the damage indicator values β_j are assumed to be random variables and are transformed into a standard normal space to scale the values. This is done to more easily determine if the beam is damaged at location j. Standard normal damage indicator values are denoted as Z_j. Hypothesis testing is used to classify the elements in one of two classes: (1) element j is undamaged; or (2) element j is damaged. A threshold value is judgmentally selected and used to determine which of the j elements are possibly damaged along the span of the beam, e.g., $Z_j > 2$ indicates damage at member j within a 95% confidence interval. Damage indicator values are transformed into standard normal space using the following equation:

$$Z_j = \frac{\beta_j - \mu_{\beta j}}{\sigma_{\beta j}} \tag{10}$$

where $\mu_{\beta j}$ = mean of β_j values for all j elements; and $\sigma_{\beta j}$ = standard deviation of β_j for all j elements.

BASELINE MODEL

For a timber structure in the field, modal parameters of the as-built or pristine structure will typically not be available. Thus, a computer model of the beam must be developed and calibrated to represent the undamaged state of the beam. To do this, an initial beam model is developed using Euler-Bernoulli beam elements and the best information available for the material properties needed. Due to the significant shear deformation in wood, the beam element stiffness matrix was modified to consider the effects of shear deformation. The element stiffness matrix k_j is given below

$$k_j = \frac{EI}{1 + 2g}\begin{bmatrix} \frac{12}{L^3} & \frac{6}{L^2} & -\frac{12}{L^3} & \frac{6}{L^2} \\ \frac{6}{L^2} & \frac{4}{L}\left(1 + \frac{g}{2}\right) & -\frac{6}{L^2} & \frac{2}{L}(1 - g) \\ -\frac{12}{L^3} & -\frac{6}{L^2} & \frac{12}{L^3} & -\frac{6}{L^2} \\ \frac{6}{L^2} & \frac{2}{L}(1 - g) & -\frac{6}{L^2} & \frac{4}{L}\left(1 - \frac{g}{2}\right) \end{bmatrix} \tag{11}$$

where g = dimensionless shear constant defined as (Weaver and Gere 1980)

$$g = \frac{6fEI}{GAL^2} \tag{12}$$

where f represents the form factor for the shape of the beam section; G is the modulus of rigidity; and A is the cross-sectional area of the beam. For rectangular cross sections, f is typically taken as 6/5.

To calibrate the beam model, stiffness properties of the model are adjusted such that the eigenfrequencies (ω^2) of the model match the corresponding eigenfrequencies of the undamaged beam as measured in the laboratory. The change in natural frequency of vibration is proportional to the square root of the change in stiffness of the beam. Thus, a relatively large amount of damage or decay is required before significant changes in frequencies will be measured (Salawu 1997). In the case of an evaluation of a possibly damaged beam where undamaged modal parameters are unavailable, the baseline model is calibrated such that the model yields the same natural frequencies of vibration as measured in the possibly damaged beam in its present state. For small magnitudes of localized damage or decay, the calibrated model should represent the dynamic response of the beam sufficiently well for the purpose intended.

The calibration process used herein to adjust the properties of the beam model is the same as that developed by Stubbs and Kim (1996a). The calibration process is described below.

To calibrate the beam model such that the calculated natural frequencies of vibration of the model match the experimentally measured natural frequencies of vibration of the structure, a sensitivity matrix F is first developed. The sensitivity matrix describes the relationship between the modifications made to the input stiffness properties of the model and their resulting effect on the eigenfrequencies (ω^2).

The sensitivity matrix F is constructed as follows. First, M eigenfrequencies for the model are determined by solving the eigenproblem for the initial model. The number of eigenfrequencies obtained M should match the number of frequencies that were able to be confidently determined in the lab or field testing. Next, a known severity of ''damage'' or a known modification is made on the first property that will be adjusted in the calibration process. For example, the property k_m is modified according to the following expression:

$$k_m^* = k_m(1 + \alpha_m) \tag{13}$$

where the asterisk denotes the modified stiffness property of the model; and α_m = fractional modification to stiffness property k_m.

If the modulus of elasticity (MOE) is desired to be changed during the calibration process, the MOE of each of the elements would be modified according to the above expression. The beam model would then be constructed as before, i.e., with the same geometry, but with the modified value for the MOE. The eigenproblem would again be solved, yielding eigenfrequencies that differed from the initial model. Fractional changes in eigenfrequencies δ_i between the initial model and the modified model for the M frequencies calculated are then determined as follows:

$$\delta_i = \left(\frac{\omega_i^2}{\omega_{i0}^2} - 1\right) \tag{14}$$

where ω_i^2 = eigenfrequency for mode i from the modified beam model; and ω_{i0}^2 = eigenfrequency for mode i for the initial beam model. The first column of the sensitivity matrix is then constructed by dividing the column of δ_i values by the severity of the modification made to property m (α_m). The above process is repeated for the number of properties that are desired to be changed in the model. When finished, the sensitivity matrix should have as many columns as stiffness-related properties to be modified in the calibration process, and as many rows as the number of natural frequencies of vibration that can be confidently measured.

In order to maintain a well-determined system, the number of properties to be changed in the model should be equal to the number of frequencies that can be confidently measured during laboratory or field testing. Additionally, an overdetermined system may help in the convergence of the calibration process. An overdetermined system can be achieved by choosing the number of properties to be modified as less than the number of frequencies that can be measured experimentally.

To make necessary modifications to the beam model, the following iterative process is used. First, a column of fractional differences in eigenfrequencies between the experimentally measured eigenfrequencies $\omega_{i\text{-exp}}^2$ and those of the initial beam model ω_{i0} are calculated as follows:

$$\Delta_i = \frac{\omega_{i\text{-exp}}^2}{\omega_{i0}^2} - 1 \tag{15}$$

where $\omega_{i\text{-exp}}^2$ = experimentally measured eigenfrequency for mode i; and, ω_{i0}^2 = eigenfrequency for the initial beam model, mode i. Modifications to be made to the beam model are given in the vector α, which is calculated as follows:

$$\alpha = F^{-1}\Delta \tag{16}$$

where F = sensitivity matrix; and Δ = vector of fractional differences in eigenfrequencies Δ_i. The vector α defines the modifications to be made to the respective properties of the model (respective according to the order with which the columns of the sensitivity matrix were constructed). The model is then reconstructed with the modifications made as given above, and the eigenvalue problem is again solved. The column of fractional changes in eigenfrequencies is again calculated, this time between the experimentally measured eigenfrequencies and those from the updated model. The α vector is again calculated to determine the next modification that should be made to the model. This process is repeated until the vectors Δ or α are nearly equal to zero, at which point the beam model should yield the same natural frequencies of vibration as the experimentally measured frequencies.

For a well-determined system where the number of modified stiffness properties of the model is equal to the number of frequencies available from experimental testing, the sensitivity matrix F will be a square matrix and can be inverted using a standard inversion process. However, for an overdetermined system, the sensitivity matrix will have more rows than columns. Therefore, the inverse is approximated using the following expression for the least-squares generalized inverse:

$$F^{-1} \cong (F^T F)^{-1} F^T \tag{17}$$

Using the calibrated baseline model, mode shapes (eigenvectors) are obtained and used in the damage indicator calculations to represent the mode shapes corresponding to the undamaged state of the beam.

ANALYTICAL VERIFICATION OF DAMAGE LOCALIZATION ALGORITHM

To demonstrate the use of the damage localization algorithm in locating damage along the span of a beam, a finite-element model was constructed and used to calculate the modal parameters needed for the undamaged and damaged states of the beam. A finite-element plane stress model was used to model the behavior of a 10.16 cm × 20.32 cm (4 in. × 8 in.) timber beam with a span of 5.08 m (200 in.). The dynamic longitudinal modulus of elasticity E_x was taken as 17.24 GPa (2.5×10^6 psi) based on the results of laboratory stress-wave tests performed on several Douglas fir timber beams. E_y and G_{xy}

were both taken as 5% of E_x to represent average values for Douglas-fir [U.S. Department of Agriculture (USDA) (1999)]. E_y is the transverse modulus of elasticity for the timber beam, i.e., the radial and tangential moduli of elasticity for wood are represented in the model as the single value E_y, and G_{xy} is the modulus of rigidity.

A frequency analysis was performed to obtain the natural frequencies of vibration and the corresponding mode shapes for the first two modes of vibration. Mode shape displacements were recorded at locations within the model that would correspond to sampling locations in an experimental test. These mode shape displacement values were used to reconstruct mode shapes using Shannon's sampling theory. The model was then ''damaged'' by removing elements from the model. Modal parameters for the damaged beam were obtained by repeating the frequency analysis. Reconstructed mode shapes were used with the damage localization algorithm to attempt to localize the damage inflicted in the model. Only the first two modes were considered to demonstrate the use of the damage localization algorithm where a limited number of modal parameters are available.

It was desired to determine the minimum severity of damage that could be correctly detected and localized in a theoretical model. Thus, for the first damage case, one element approximately 6.4 mm × 6.4 mm (1/4 in. × 1/4 in.) in size was removed from the tension face at the quarter-point of the beam near the pin support to simulate a very small magnitude of damage. Successive damage cases were then simulated by removing more elements from the tension face at the quarter-point to note any trends in the detection of damage with progressive severity of simulated damage. Multiple locations of inflicted damage were also analyzed to verify the use of the algorithm in locating damage at more than one location along the span.

As discussed previously, hypothesis testing was used to determine where the damage indicator values show damage along the span. For each of the damage cases below, the confidence interval was set such that $Z_j > 2$ indicates damage (corresponding to approximately 95% confidence).

Elements removed for each of the damage cases are given in Table 1. The location of the removed elements is given as the distance away from the pin support, expressed as a fraction of the span of the beam model. For example, the 1/4-point would be located at a distance equal to 1/4 of the span away from the pin support. The 3/4-point would then be located at a distance equal to 3/4 of the span away from the pin support, or at the 1/4-point adjacent to the roller support for the simply supported beam model. It should be noted that two different models were used in the analytical verification. The model used for damage cases 1 and 2 used a refined mesh near the 1/4-point from the pin support so that a small magnitude of damage could be inflicted. The model used for damage cases 3–7 used a uniform mesh of elements approximately 25.4 mm × 25.4 mm (1 in. × 1 in.) in size.

TABLE 1. Simulated Damage for Analytical Verification

Damage case (1)	No. of elements removed (2)	Damage Size: Width mm (in.) (3)	Damage Size: Depth mm (in.) (4)	Location (5)
1	1	6.4 (0.25)	6.4 (0.25)	1/4-Point
2	2	6.4 (0.25)	12.7 (0.50)	1/4-Point
3	1	25.4 (1.00)	25.4 (1.00)	1/4-Point
4	2	25.4 (1.00)	50.8 (1.00)	1/4-Point
5	3	25.4 (1.00)	76.2 (3.00)	1/4-Point
6	3	25.4 (1.00)	76.2 (3.00)	1/4-Point
6	4	25.4 (1.00)	101.6 (4.00)	5/8-Point
7	3	25.4 (1.00)	76.2 (3.00)	1/4-Point
7	4	25.4 (1.00)	101.6 (4.00)	Midspan

Changes in natural frequencies of vibration for the first two modes of vibration for each of the damage cases are given in Table 2. It is seen in Table 2 that the frequencies for the undamaged models differ slightly from each other. This is due to the different meshes used to construct the model. For damage cases 1 and 2, the undamaged modal parameters used in the damage localization algorithm were obtained using the undamaged model 1. For damage cases 3–7, the undamaged modal parameters used in the damage localization algorithm were obtained using the undamaged model 2.

The statistically normalized damage indicator values (Z_j) for each of the first five damage cases are shown in Figs. 1–5. It can be seen in these figures that the magnitude of the damage indicator values at the location of damage increases with increasing severity of damage. Consequently, the confidence in

TABLE 2. Shifts in Natural Frequencies of Vibration of Analytical Model

Model (1)	Damage case (2)	ω_1 (Hz) (3)	ω_2 (Hz) (4)
1	Undamaged	13.186	49.863
1	1	13.179	49.813
1	2	13.145	49.576
2	Undamaged	13.165	49.600
2	3	13.047	48.809
2	4	12.680	46.604
2	5	11.964	43.185
2	6	9.277	37.110
2	7	8.958	43.260

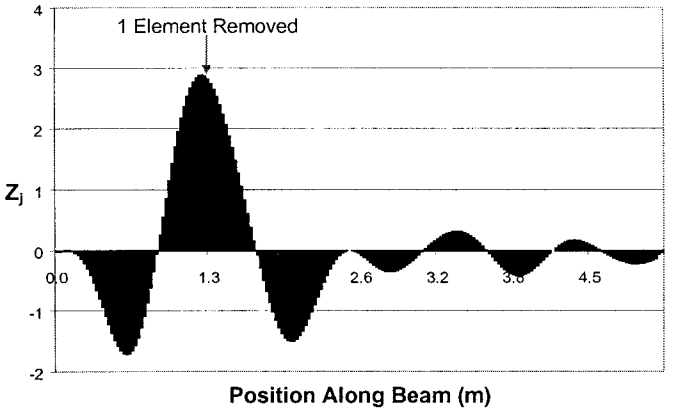

FIG. 1. Damage Indicator Values for Damage Case 1 (Modes Considered: 1 and 2)

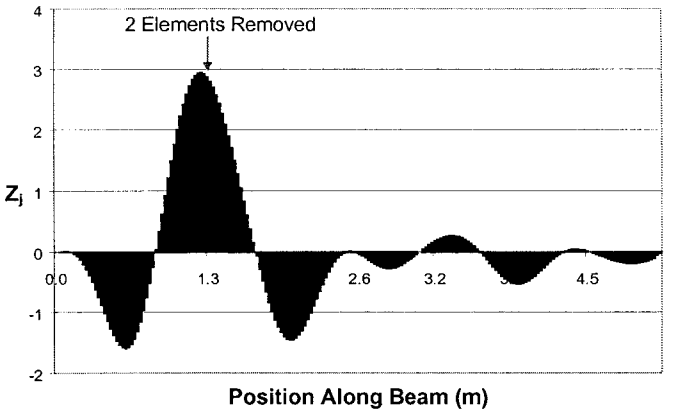

FIG. 2. Damage Indicator Values for Damage Case 2 (Modes Considered: 1 and 2)

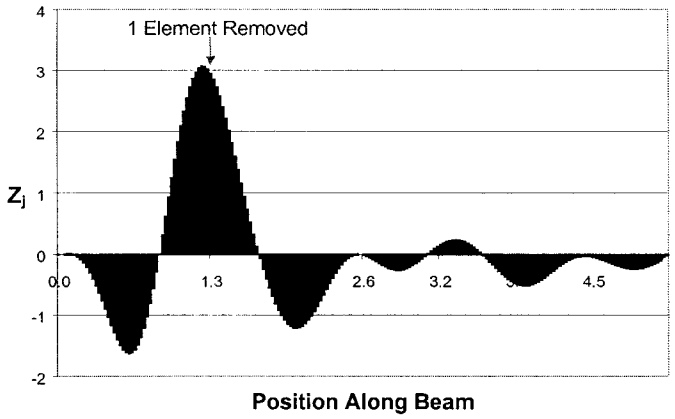

FIG. 3. Damage Indicator Values for Damage Case 3 (Modes Considered: 1 and 2)

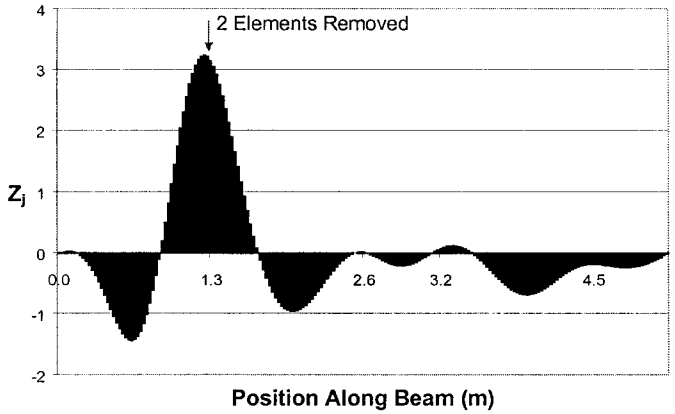

FIG. 4. Damage Indicator Values for Damage Case 4 (Modes Considered: 1 and 2)

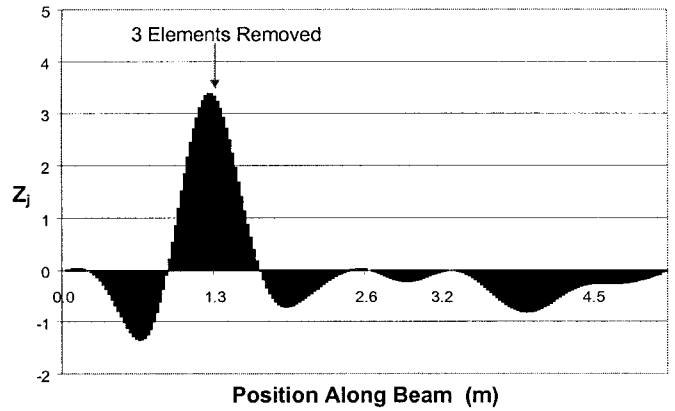

FIG. 5. Damage Indicator Values for Damage Case 5 (Modes Considered: 1 and 2)

detecting the damage using the localization algorithm increases with increasing severity of damage. The noted trend is similar to the conclusions found in previous studies where the damage localization algorithm was used to estimate the severity of damage at identified locations in steel plate girders (Stubbs et al. 1998) and space truss models (Park and Stubbs 1996).

As noted in Table 1, damage case 6 consisted of simulated damage at both the 1/4-point and the 5/8-point. The analysis was performed for this damage case to test the damage localization algorithm in locating damage at more than one location within the beam. Given the elements already removed at the 1/4-point from damage case 5, elements were removed from the tension face at the 5/8-point, one at a time, until the damage at both locations could be detected. Both locations of damage could not be detected simultaneously until the severity of damage at the 5/8-point consisted of four removed elements. The variation in damage indicator values for damage case 6 is shown in Fig. 6.

It was noted during the evaluation of the damage localization algorithm that the higher modes had a dominating contribution to the damage indicator values when each of the experimentally obtained modes were considered as defined by (9). To test the algorithm performance in detecting damage at a location where only the first mode should correctly locate the damage, an additional analytical evaluation was performed. For damage case 7, the damage already inflicted in damage case 5 was used in combination with the removal of four el-

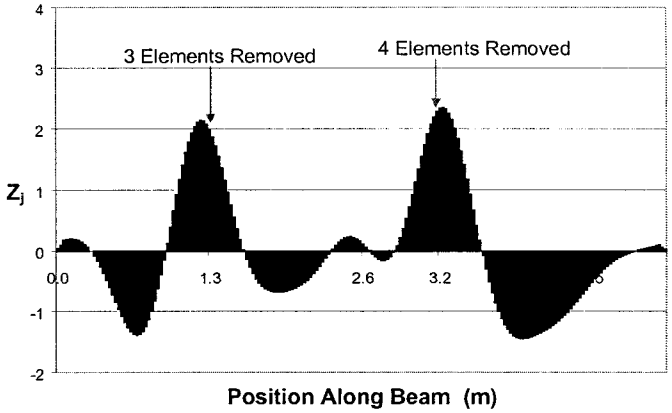

FIG. 6. Damage Indicator Values for Damage Case 6 (Modes Considered: 1 and 2)

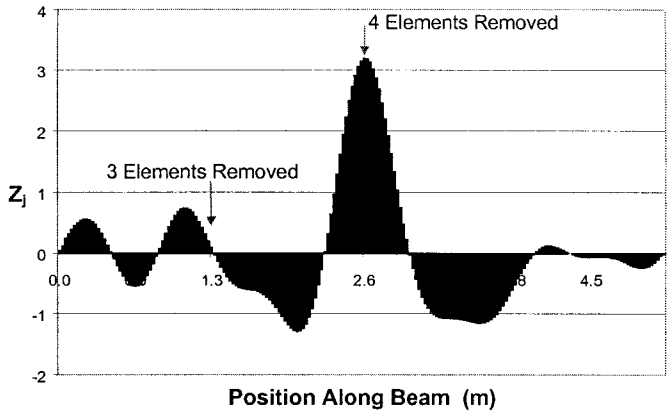

FIG. 7. Damage Indicator Values for Damage Case 7 (Mode Considered: 1)

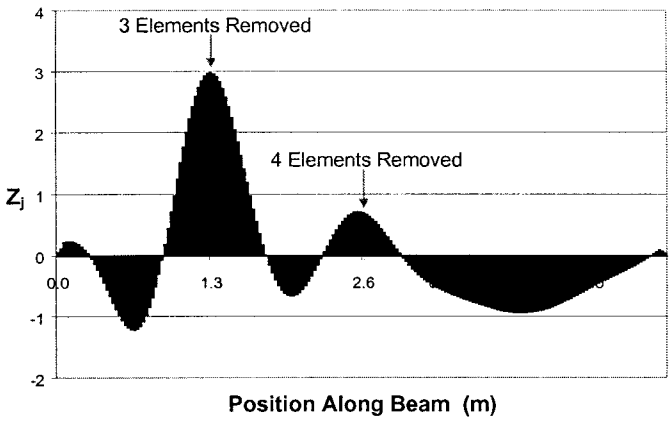

FIG. 8. Damage Indicator Values for Damage Case 7 (Modes Considered: 1 and 2)

ements from the tension face at midspan. Since mode shape 2 has a node at midspan, only mode shape 1 should detect the stimulated damage at midspan. The question here is whether or not both locations of damage can be detected when the contributions from modes 1 and 2 are combined as per (9). Variation in damage indicator values from both the contribution of mode 1 alone as well as from the contribution of the first two modes is shown in Figs. 7 and 8, respectively.

From Fig. 8, it is seen that the localization algorithm, when using the combination of the first two modes, is unable to detect the damage at both locations simultaneously. This is largely due to the fact that the contribution to the damage indicator values from mode 2 dominates the contribution from mode 1. In fact, the damage indicator variation shown in Fig. 8 looks essentially identical to the damage indicator variation when considering mode 2 alone. As shown in Fig. 7 when only mode 1 is considered, the damage at the midspan is detected and correctly located, but the damage at the quarter-point cannot be detected. Thus, the mode shapes selected to be used in the damage localization algorithm should be selected according to the location of the damage. To correctly detect multiple or unknown locations of damage within the beam, it may be necessary to consider the damage indicator variation for each mode individually as well as the variation corresponding to the combination of modes.

CONCLUSIONS

In this paper, a technique to conduct experimental modal analysis was developed, a damage localization algorithm was presented, and an analytical evaluation was conducted to determine the sensitivity of the algorithm to various cases of simulated damage in a plane-stress simply supported beam model. For the results of the analytical verification of the damage localization algorithm, it can be concluded that the algorithm can identify the location of even small magnitudes of simulated damage within a beam model. Noted trends in which the standard normal damage indicator values increase in magnitude with increasing severity of simulated damage show that the algorithm has the potential to also predict the severity of the identified damage. For multiple or unknown locations of damage, each of the mode shapes available should be considered separately as well as combined to best identify all possible locations of damage.

In the second part of this two-part paper, the developed method of global nondestructive evaluation will be verified experimentally through laboratory tests performed on simply supported timber beams.

ACKNOWLEDGMENTS

Funding for this project was provided by the U.S. Federal Highway Administration and the USDA Forest Service Forest Products Laboratory. The writers wish to thank Dr. Robert Ross of the Forest Products Laboratory for his assistance on the project as well as Dr. Sooyong Park at Texas A&M University for his suggestions concerning the implementation of the damage localization algorithm for use in timber beams.

APPENDIX I. REFERENCES

Aktan, A. E., et al. (1992). ''Nondestructive and destructive testing of a reinforced concrete slab bridge and associated analytical studies.'' *Rep. No. UC-CII 92/02*, Ohio Department of Transportation.

Alampalli, S., Fu, G., and Aziz, I. A. (1992). ''Modal analysis as a bridge inspection tool.'' *Proc., 10th Int. Modal Anal. Conf.*, Vol. 2, 1359–1366.

Bolton, R., Stubbs, N., Park, S., and Choi, H. (1998). ''Analysis of Lavic Road overcrossing field data.'' Engrg. Technol. Dept., Texas A&M University, College Station, Tex.

Emerson, R. N., Pollock, D. G., Kainz, J. A., Fridley, K. J., McLean, D. I., and Ross, R. J. (1998). ''Nondestructive evaluation techniques for timber bridges.'' *Proc., 1998 World Conf. on Timber Engrg. (WCTE)*, Presses Polytechniques et Universitaires Romandes, 670–677.

Halvorsen, W. G., and Brown, D. L. (1977). ''Impulse technique for structural frequency response testing.'' *Sound and Vibration*, Nov.

Inman, D. J. (1996). *Engineering vibration*, Prentice-Hall, Englewood Cliffs, N.J.

Mazurek, D. F., and DeWolf, J. T. (1990). ''Experimental study of bridge monitoring technique.'' *J. Struct. Engrg.*, ASCE, 116(9), 2532–2549.

Park, S., and Stubbs, N. (1995). ''Reconstruction of mode shapes using Shannon's sampling theorem and its application to the nondestructive damage localization algorithm.'' *Proc., SPIE, Smart Struct. and Mat. 1995*, Vol. 2446, 280–292.

Park, S., and Stubbs, N. (1996). ''Bridge diagnostics via vibration monitoring.'' *Proc., SPIE, Smart Struct. and Mat. 1996*, Vol. 2719, 36–45.

Peterson, S. T., et al. (2001). ''Application of dynamic system identification to timber beams. II.'' *J. Struct. Engrg.*, ASCE, 127(4), 426–432.

Raghavendrachar, M., and Aktan, A. E. (1992). ''Flexibility by multi-reference impact testing for bridge diagnostics.'' *J. Struct. Engrg.*, ASCE, 118(8), 2186–2203.

Salawu, O. S. (1997). ''Detection of structural damage through changes in frequency: A review.'' *Engrg. Struct.*, 19(9), 718–723.

Stubbs, N., and Garcia, G. (1996b). ''Application of pattern recognition to damage localization.'' *Microcomputers in Civ. Engrg.*, 11, 395–409.

Stubbs, N., and Kim, J. T. (1996a). ''Damage localization in structures without baseline modal parameters.'' *AIAA J.*, 34(8), 1644–1649.

Stubbs, N., Kim, J. T., and Farrar, C. R. (1995). ''Field verification of a nondestructive damage localization and severity estimation algorithm.'' *Proc., 13th Int. Modal Anal. Conf.*, 210–218.

Stubbs, N., and Park, S. (1996c). ''Optimal sensor placement for mode shapes via Shannon's sampling theorem.'' *Microcomputers in Civ. Engrg.*, 11, 411–419.

Stubbs, N., Park, S., and Sikorski, C. (1997). ''A general methodology to nondestructively evaluate bridge structural safety.'' *Tech. Rep. No. NDD 04-97-04 Submitted to State of California, Department of Transportation, Sacramento, Calif.*, Texas Engrg. Experimental Station, Texas A&M University, College Station, Tex.

Stubbs, N., Sikorsky, C., Park, S., Choi, S., and Bolton, R. (1998). ''A methodology to nondestructively evaluate the structural properties of bridges.'' *Proc., 5th CALTRANS Seismic Res. Workshop*, California Department of Transportation Service Center.

U.S. Department of Agriculture (USDA). (1999). ''Wood handbook: Wood as an engineering material.'' *General Tech. Rep. FPL-GTR-113*, Forest Product Laboratory, Madison, Wis.

Weaver, W., and Gere, J. (1980). *Matrix analysis of framed structures*, 2nd Ed., Van Nostrand Reinhold, New York.

APPENDIX II. NOTATION

The following symbols are used in this paper:

E_x, $E(x)$ = longitudinal modulus of elasticity;
E_y = transverse modulus of elasticity;
F = sensitivity matrix;
F_{ij}, F_{ij}^* = fraction of modal strain energy concentrated in element j for mode i;
F_s = sampling frequency;
f = form factor for shear constant;
G, G_{xy} = modulus of rigidity;
$G_u(\omega)$ = power spectrum of $u(t)$;
$G_{uv}(\omega)$ = cross spectrum between $u(t)$ and $v(t)$;
g = shear constant;
$H(\omega)$ = frequency response spectrum;
I = second moment of area;
i = natural frequency of vibration, mode;
j = element;
k_j = element stiffness matrix for element j;
k_m = stiffness property to be modified;
L = span length;
n = number of coordinates in mode shape vectors;
$S(nT)$ = experimentally measured mode shape coordinate at position nT;
$S(x)$ = interpolated mode shape coordinate at position x;
T = spacing of experimentally measured mode shape coordinates;
U_{ij}, U_{ij}^* = modal strain energy for mode i, element j;
Z_j = standard normal damage indicator value for element j;

α = vector of fractional stiffness modification values;
α_m = fractional stiffness modification value for stiffness property m;
β_{ij} = damage indicator value for mode I, element j;
Δ = vector of fractional changes in eigenfrequencies;
Δ_i, δ_i = fractional changes in eigenfrequencies for mode i;
ϕ_{Ej} = mode shape coordinate for experimental mode shape, element j;
ϕ_i = mode shape vector corresponding to mode of vibration i;
ϕ_{ij} = mode shape coordinate for mode i, element j;
ϕ_{Tj} = mode shape coordinate for theoretical mode shape, element j;
$\mu_{\beta j}$ = mean of β_j values for all j elements;
$\sigma_{\beta j}$ = standard deviation of β_j values for all j elements;
ω_c = cutoff frequency;
ω_i = natural frequency of vibration for mode i;
$\omega^2_{i\text{-exp}}$ = experimentally measured eigenfrequency for mode i, and
ω^2_{i0} = eigenfrequency for initial beam model, mode I.